Experimental evidence of the spin-glass transition in the diluted magnetic semiconductor $Zn_{1-x}Mn_xIn_2Se_4$

2008 J. Phys.: Condens. Matter 20 455211

(http://iopscience.iop.org/0953-8984/20/45/455211)

J. Phys.: Condens. Matter **20** (2008) 455211 (7pp) doi:10.1088/0953-8984/20/45/455211

Experimental evidence of the spin-glass transition in the diluted magnetic semiconductor $Zn_{1-x}Mn_xIn_2Se_4$

J Mantilla[1], E Ter Haar[2], J A H Coaquira[3] and V Bindilatti[2]

[1] Laboratório de Física Molecular, Universidad Central de Venezuela, Caracas 1040, Venezuela
[2] Instituto de Física, Universidade de São Paulo, CP 66318, 05315-970, São Paulo, Brazil
[3] Instituto de Física, Universidade de Brasília, CP 04455, 70910-900, Brasília, Brazil

E-mail: jmantilla@fisica.ciens.ucv.ve

Received 11 April 2008, in final form 6 August 2008
Published 13 October 2008
Online at stacks.iop.org/JPhysCM/20/455211

Abstract

This work reports on magnetic measurements of the quasi-two-dimensional (quasi-2D) system $Zn_{1-x}Mn_xIn_2Se_4$, with $0.01 \leqslant x \leqslant 1.00$. For $x > 0.67$, the quasi-2D system seems to develop a spin-glass behaviour. Evidence of a true phase transition phenomenon is provided by the steep increase of the nonlinear susceptibility χ_{nl} when approaching T_C from above. The static scaling of χ_{nl} data yields critical exponents $\delta = 4.0 \pm 0.2$, $\phi = 4.37 \pm 0.17$ and $T_C = 3.4 \pm 0.1$ K for the sample with $x = 1.00$ and similar values for the sample with $x = 0.87$. These critical exponents are in good agreement with values reported for other spin-glass systems with short-range interactions.

(Some figures in this article are in colour only in the electronic version)

1. Introduction

Dilute magnetic semiconducting (DMS) systems with controlled amounts of magnetic elements have received considerable attention due to the interactions of interest that occur between their electronic and magnetic subsystems. The II–VI systems containing Mn [1, 2] are well known, and the more complex ternary and quaternary systems have been subjects of recent structural and magnetic studies [3] aiming to explore and manipulate the electronic, magnetic and structural interactions. An example is provided by the cationic disorder, which can be studied via its effects on the magnetic properties [4, 5].

The spin-glass behaviour in DMS with short-range antiferromagnetic interactions has been studied for a long time, but its relation to their canonical spin-glass counterpart is still under investigation [6–8]. The variety of experimental realizations of spin-glass state is due to different forms in which the two main ingredients, randomness and frustration, are present [9, 10]. In fact, a random distribution of magnetic interactions can be achieved either by topological disorder or by mixing different kinds of magnetic ions; it can also be generated by short-range interactions [11, 12].

Here, we report on the magnetic properties of other site-disordered semiconductors with a short-range antiferromagnetic superexchange interaction between Heisenberg spins but with a quasi-two-dimensional structure: $Zn_{1-x}Mn_xIn_2Se_4$. For Mn concentration of $x \geqslant 0.87$, as was established by Range *et al* [13] and confirmed by us [14], this structure consists of slabs of four Se layers which are van der Waals coupled to each other. Within the slabs the metal cations are distributed over three triangular layers between the Se layers, in a tetrahedral–octahedral–tetrahedral site sequence.

The Mn^{+2} ions provide a localized, pure spin magnetic moment ($S = 5/2$) and interact through short-range antiferromagnetic superexchange. For Mn ions in the tetrahedral layers the exchange paths are similar to those of zinc-blende II–VI DMS which have an exchange constant J of the order -12 K.

In this work we have investigated the static properties of the spin freezing phenomenon observed in the $Zn_{1-x}Mn_xIn_2Se_4$ system by means of dc magnetic susceptibility measurements.

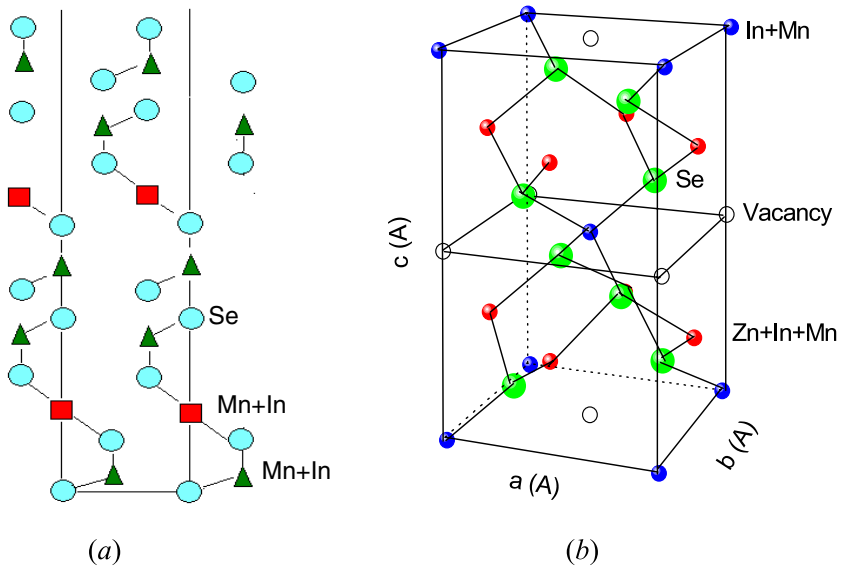

Figure 1. (a) Unit cell of the $MnIn_2Se_4$ compound (space group $R\bar{3}m$) reproduced from [16]. The cations are distributed randomly in octahedral (■) and tetrahedral sites (▲). (b) Unit cell of the $ZnIn_2Se_4$ compound (space group $I\bar{4}2m$) reproduced from [16]. The cations are also randomly distributed in octahedral and tetrahedral sites.

2. Experimental details

$Zn_{1-x}Mn_xIn_2Se_4$ samples with nominal Mn concentrations $0.01 \leqslant x \leqslant 1.00$ were prepared by a vapour phase chemical transport technique (CVT) [14–16]. A detailed explanation of the growth procedure is given in [14] and [16]. The analysis of Mn content was determined by energy dispersive x-ray fluorescence spectroscopy (EDX) with a Shimadzu EDX-900 device. The Mn concentrations determined from EDX data are in good agreement with those extracted from magnetic measurements [16, 17]. Room-temperature x-ray power-diffraction patterns indicate the formation of a pure rhombohedral structure [13] (space group $R\bar{3}m$) for samples with $x \geqslant 0.87$ (see figure 1(a)) and a pure tetragonal structure (space group $I\bar{4}2m$) (see figure 1(b)) for samples with $x \leqslant 0.25$ [16]. In the intermediate region ($0.25 < x < 0.87$) the coexistence of both crystalline phases has been determined as reported in [16]. X-ray Laue-diffraction experiments (not shown here) indicate the formation of plate-like single crystals of rhombohedral structure for samples with $x = 1.00$ ($MnIn_2Se_4$) and $x = 0.87$, the growth direction of which is determined to be along the c-axis. The Laue pattern of the sample with $x = 0.67$ also shows the symmetry expected for the rhombohedral phase, but our measurements indicate a superposition of several crystals, each with a different c-axis orientation [16]. The Laue pattern of the sample with $x = 0.25$ shows the formation of plate-like single crystals of tetragonal structure with a growth direction along [112] (see [16]). These findings indicate the formation of plate-like single crystals for $x \leqslant 0.25$ and $x \geqslant 0.87$ and samples with poor crystallinity (i.e. a mixture of rhombohedral and tetragonal phases) for the range $0.25 < x < 0.87$.

Magnetic measurements were performed in a commercial superconducting quantum interference device magnetometer in both zero-field-cooling (ZFC) and field-cooling (FC) modes, in the range $2\ \text{K} \leqslant T \leqslant 300\ \text{K}$ and applied fields up to 70 kOe (7 T). In order to carry out the measurements, the plate-like single crystals (samples with $x \leqslant 0.25$ and $x \geqslant 0.87$) and the multiple crystals (samples with $0.25 < x < 0.87$) were powdered before use. In all cases, the diamagnetic contribution of the sample holder was subtracted, and the resulting susceptibility was further corrected for core diamagnetism of the ions.

3. Results and discussion

In figure 2 we show the temperature dependence of the dc magnetic susceptibility χ_{dc} measured in the ZFC mode with $H = 100$ Oe and in the temperature range from 4.0 K to room temperature for $Zn_{1-x}Mn_xIn_2Se_4$ compounds. Depending on the Mn concentration, two different regions can be distinguished. Samples with lower Mn content ($x < 0.60$) show a paramagnetic behaviour in the whole temperature range. However, samples with $x \geqslant 0.67$ show a paramagnetic behaviour in the region of $T > 150$ K and the susceptibility data deviate from the Curie behaviour when T is decreased below 150 K. This behaviour is associated with the onset of magnetic correlations between Mn ions [18, 19]. When the temperature is further decreased, a peak in the ZFC curve is observed. The peak position appears at $T_m = 3.5$, 3.0, 2.5 K for samples with $x = 1.00$, 0.87 and 0.67, respectively. These features are associated with fingerprints of a spin-glass-like behaviour. The Mn concentration $x \sim 0.67$ seems to separate two different magnetic regimes established in the $Zn_{1-x}Mn_xIn_2Se_4$ system.

3.1. Paramagnetic regime

In order to assess the magnetic properties of the $Zn_{1-x}Mn_xIn_2Se_4$ compounds when the Mn concentration is varied, the

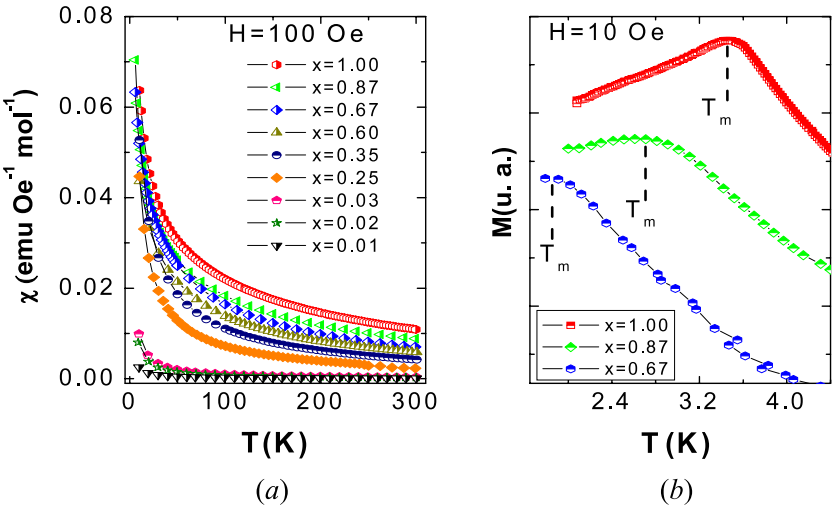

Figure 2. (a) Temperature dependence of the dc magnetic susceptibility of the $Zn_{1-x}Mn_xIn_2Se_4$ samples. (b) Magnification of the low-temperature region of the ZFC curves carried out with $H_{dc} = 10$ Oe.

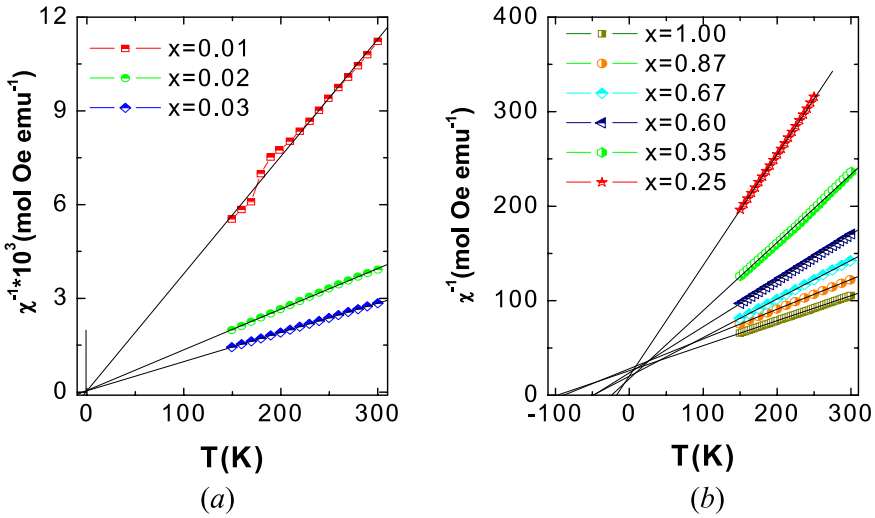

Figure 3. Temperature variation of the inverse of the magnetic susceptibility ($\chi^{-1}(T)$) of $Zn_{1-x}Mn_xIn_2Se_4$ samples in the paramagnetic regime ($T \geqslant 150$ K). (a) For samples with $x \leqslant 0.03$ and (b) for samples with $x \geqslant 0.25$. The lines represent the fits and their extrapolation towards the negative-temperature axis provides the paramagnetic Curie temperature, $\Theta(x)$.

inverse of the susceptibilities in the high-temperature region are plotted in figure 3. As mentioned above, all samples display a typical Curie–Weiss behaviour in this high-temperature region.

We have analysed the data above 150 K using the Curie–Weiss law given by [19, 20]:

$$\chi^{-1}(T) = \frac{T - \Theta(x)}{C(x)} \tag{1}$$

where C is the Curie constant and Θ is the paramagnetic Curie temperature. The experimental data are well reproduced by equation (1) in the high-temperature ($T \geqslant 150$ K) region, as shown in figure 3.

From the fit, an effective magnetic moment of $\mu_{eff} = 5.88\ \mu_B$ was determined for the sample with $x = 1.00$. This value is comparable to the one expected for spin-only magnetic moment of Mn ions with $S = 5/2$ ($\mu_{eff} = 5.92\ \mu_B$), which confirms the presence of mainly Mn^{2+} ions in the system. The ∼7% of difference can be assigned either to the p–d admixture of Mn^{2+} and anion ions or to the occurrence of a small population of Mn^{3+} ions [21].

It is worth noting that, for samples with a low Mn concentration ($x \leqslant 0.03$), all χ^{-1} versus T curves in figure 3(a), extrapolated from the high-temperature region intercept at the same height in $T = 0$ K independently of x [19]. Table 1 lists the Mn concentration (x) determined from the Curie constant values obtained from the fit for the whole set of samples. These x_{mag} values have been determined using the relation: $C(x) = \frac{S(S+1)g^2\mu_B^2 N_A}{3k_B}x = C_0 x$, where N_A is the Avogadro number and C_0 is the Curie constant of the spin-only magnetic moment of Mn ions ($S = 5/2$) [19–21]. These x_{mag} values are in good agreement with the values determined from EDX measurements. An estimate of the

Table 1. Collection of Mn concentrations and magnetic parameters obtained from dc magnetic measurements for $Zn_{1-x}Mn_xIn_2Se_4$ samples. T_m is the freezing temperature and Θ is the paramagnetic Curie temperature.

x (nominal)	x (EDX)	x (Magn)	μ_{eff} (μ_B)	T_m (K)	Θ (K)
1.00	1.00	1.00	5.88 ± 0.02	3.52 ± 0.05	-96 ± 5
0.9	0.86 ± 0.01	0.87 ± 0.02	5.80 ± 0.02	2.9 ± 0.1	-86 ± 5
0.7	0.68 ± 0.02	0.67 ± 0.02	4.45 ± 0.03	2.0 ± 0.1	-49 ± 2
0.60	0.65 ± 0.01	0.60 ± 0.01	4.05 ± 0.03	<1.8	-47 ± 2
0.40	0.29 ± 0.03	0.35 ± 0.03	3.36 ± 0.03	<1.8	-22 ± 3
0.30	0.21 ± 0.01	0.25 ± 0.03	2.60 ± 0.04	<1.8	-14 ± 3
0.03	0.028 ± 0.004	0.031 ± 0.002	0.93 ± 0.05	<1.8	-4.5 ± 0.3
0.02	0.021 ± 0.002	0.021 ± 0.002	0.79 ± 0.05	<1.8	-2.1 ± 0.3
0.01	0.014 ± 0.003	0.011 ± 0.002	0.46 ± 0.05	<1.8	-1.8 ± 0.3

effective magnetic moments has been obtained using the Curie constant and the nominal values of x. Even when some of the magnetic moments show some discrepancies when compared to the relation $\mu_{\text{eff}} = 5.92\sqrt{x}(\mu_B)$ [19], the whole set of data is well described by that relation and the discrepancies are associated with the differences between the nominal and the experimental value of x. Negative values of Θ are obtained for the whole set of samples and they show a linear decrease with x, being more negatives when more Mn is present in the sample (see table 1). The set of values is well represented by the relation $\Theta(x) = (-90 \pm 4)x$. On the other hand, the negative values of Θ suggest that the dominant interactions between Mn magnetic moments are antiferromagnetic in nature. These values of Θ are in good agreement with those obtained from electron paramagnetic resonance (EPR) which were reported in a previous work [22].

3.2. Spin freezing regime

As previously reported (reference [22]), the temperature dependence of the low-field (100 Oe) ZFC and FC traces obtained for samples with $x \geqslant 0.87$ exhibit quite a similar behaviour, namely, a sharp peak in the ZFC curves (see figure 2(b)) and a pronounced ZFC–FC irreversibility below the cusp. These features are evidences of collective spin freezing. As mentioned above, the negative values of the paramagnetic Curie temperature (ranging from -86 to -96 K) make evident the existence of dominant antiferromagnetic interactions in samples with $x \geqslant 0.87$ [17]. The cusp position (T_m) indicated in figure 2(b) decreases as the Mn concentration is increased and their values are in good agreement with those obtained from EPR measurements [22].

In order to discuss in more detail the spin-glass behaviour and its relation with the crystal phase, table 2 presents the average interatomic cation–anion distances determined from XRD data analysis. Average distances of the rhombohedral phase show a smooth tendency to decrease when the Mn ion is substituted by Zn ions. Almost constant values of the average distances for the tetragonal phase are determined. It seems that the difference in ionic radii between Zn^{2+} and Mn^{2+} ions (0.74 and 0.80 Å in tetrahedral sites, respectively) should produce the decreasing tendency of the interatomic distances in the rhombohedral phase and should drive to the crystalline phase transition from the rhombohedral to the tetragonal phase. On the other hand, both structures show the characteristic random

Table 2. Average anion–cation interatomic distances for the tetragonal and rhombohedral phases in $Zn_{1-x}Mn_xIn_2Se_4$ determined from XRD data.

x	Tetragonal ($I\bar{4}2m$) Mn/Zn–Se (Å)	Rhombohedral ($R\bar{3}m$) Mn/Zn–Se (Å)
0.01	2.532	
0.25	2.537	
0.35	2.534	
0.60		2.559
0.67		2.564
0.87		2.568
1.00		2.569

distribution of Mn and Zn ions over the accessible tetrahedral and octahedral sites [21, 23]. This random distribution of Mn ions and the occurrence of vacancies should drive to disordered magnetic interactions (breaking superexchange Mn–Se–Mn paths) and provides a source for the spin-glass behaviour observed in this DMS compound. Spin-glass behaviour arising from a topological disorder has been reported for several (Mn, II)–III_2–VI_4 systems, irrespective of the crystalline phase [21, 24, 25].

In a previous work [26], evidences of true spin-glass transition was determined from dynamic measurements (AC susceptibility). The maximum of the in-phase magnetic susceptibility (T_f) shows a relative variation per frequency decade of $(\Delta T_f/T_f)/\Delta \log f \approx 0.022$. This ratio is intermediate between those typically reported values for canonical spin glasses (0.7×10^{-2}) [9] and for the insulator, $Eu_{0.6}Sr_{0.4}S$ (5×10^{-2}) [27]. However, the value determined for $Zn_{1-x}Mn_xIn_2Se_4$ is consistent with commonly reported values for other spin glasses [21, 28], irrespective of the crystalline structure of those spin-glass systems. Study of the dynamic properties has provided us with critical exponents which are consistent with those reported for other spin-glass *like* systems [26].

In order to get more evidence of the true spin-glass transition happening in $Zn_{1-x}Mn_xIn_2Se_4$ compounds, the dependence of FC magnetic susceptibility (χ) as a function of both temperature and applied magnetic field is used to study the static critical behaviour of the system. In figure 4 we depict dc susceptibility curves for samples with $x = 0.87$ and 1.00 carried out in the range from 2 to 10 K with the dc field varying from 20 to 2000 Oe. As observed in the plot (see figure 4), the effect of the nonlinear terms is

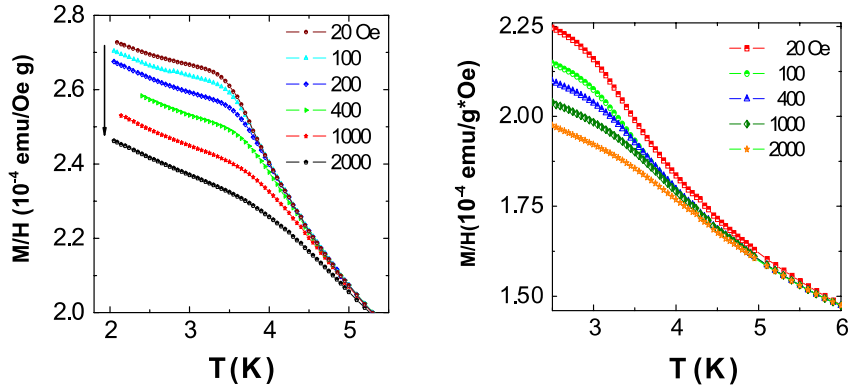

Figure 4. Temperature dependence of the field-cooled magnetization obtained with different magnetic fields for the $Zn_{1-x}Mn_xIn_2Se_4$ compound. The left-hand plot is for $x = 1.0$ and the right-hand one for $x = 0.87$.

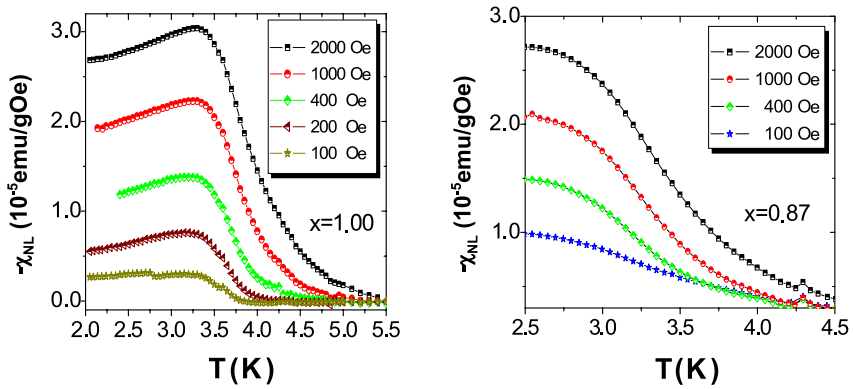

Figure 5. Temperature dependence of the nonlinear susceptibility for $Zn_{1-x}Mn_xIn_2Se_4$ samples with Mn composition $x = 0.87$ and 1.00.

manifested through the broadening of the peak associated with the spin freezing phenomena when the magnetic field is increased. The nonlinear contribution to the total magnetic susceptibility shows a divergent tendency when approaching the critical temperature from above, as shown in figure 5. Similar behaviour has been reported for other spin-glass systems [21, 28–33]. This divergent behaviour has been interpreted as evidence for the true spin-glass transition.

To study the nature of the transition that takes place at T_m we have additionally analysed the nonlinear part of the magnetic susceptibility. The nonlinear susceptibility, $\chi_{nl}(T, H)$, of a specimen is given by [34]:

$$\chi_{nl}(T, H) = \chi_1(T) - M(T, H)/H, \tag{2}$$

where $\chi_1(T)$ is the linear susceptibility derived as described in [33] and [34] and $M(T, H)$ is the measured magnetization of the specimen.

Since the linear component, $\chi_1(T)$, is non-divergent and if a true thermodynamic phase transition occurs near to T_m, then the first two nonlinear terms should diverge as $(T - T_c)^{-\gamma}$ and $(T - T_c)^{-2(\gamma+\beta)}$, respectively [28].

In the critical region, it is expect that $\chi_{nl}(T, H)$ follows the universal scaling relation [34–37]:

$$\chi_{nl}(H, T) \propto H^{2/\delta} f\left(\frac{t}{H^{2/\phi}}\right). \tag{3}$$

In equation (3) the reduced temperature is defined as $t = (T - T_c)/T_c$, δ and ϕ are the critical exponents, T_c is the critical temperature and $f(z)$ is the scaling function that satisfies [38]:

$$f(z) = \text{const}, \quad z \Rightarrow 0$$

$$f(z) = z^{-\gamma}, \quad z \Rightarrow \infty.$$

The critical exponent δ can therefore be obtained from the asymptotic behaviour when x goes towards zero [39]. The curve obtained from the experimental data is displayed as a log–log scale plot in figure 6 for the region of $T > T_m$. Values of T_C and the critical exponents (ϕ and δ) were varied in order to obtain the optimum data collapsing shown in figure 6.

The best scaling of experimental data has been obtained with the following set of critical exponents: $\delta = 4.0 \pm 0.2$, $\phi = 4.3 \pm 0.2$ and $T_C = 3.4 \pm 0.1$ K, for the sample with $x = 1.00$; and $\delta = 4.2 \pm 0.2$, $\phi = 4.5 \pm 0.2$ and $T_C = 2.6 \pm 0.1$ K, for the sample with $x = 0.87$. These critical exponents (δ and ϕ) are consistent with critical exponents reported for the AgMn [39] and the $Zn_{1-x}Mn_xIn_2Te_4$ compound [21]. Similar critical exponents of three-dimensional (3D) spin glasses with short-range interactions obtained from numerical calculations were reported in [40] and [41]. Higher critical exponents have been reported for the ceramic $BaCo_6T_6O_{19}$, which shows reduced spin dimensionality due to planar anisotropy [32]. Recently,

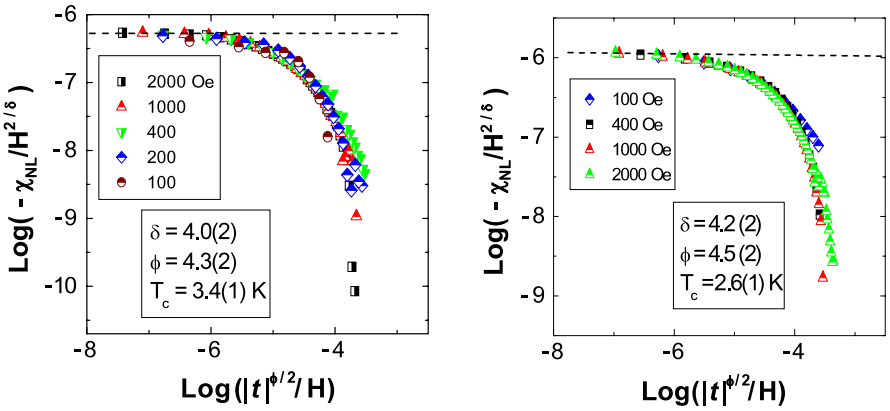

Figure 6. Scaling plot of the nonlinear part of the susceptibility for $Zn_{1-x}Mn_xIn_2Se_4$ samples with composition $x = 1.00$ (on the left-hand side) and $x = 0.87$ (on the right-hand side). The plots have been obtained according to the universal scaling function given by equation (3).

a true spin-glass transition was reported for the quasi-two-dimensional $Ga_{1-x}Mn_xS$ system [24] whose critical exponents are consistent with 3D systems. These results suggest that the system studied in this work ($Zn_{1-x}Mn_xIn_2Se_4$) with $x \geqslant 0.87$, where the cations are randomly distributed over a layered cation lattice (a quasi-two-dimensional system) with short-range antiferromagnetic superexchange interactions, belongs to the same universality as 3D spin glasses.

4. Conclusions

DC magnetic susceptibility for samples of $Zn_{1-x}Mn_xIn_2Se_4$, covering a wide range of Mn concentrations has been investigated in this work. The Mn concentration (x) and the paramagnetic Curie parameter (Θ), estimated from the high-temperature magnetic data ($T > 150$ K), are in good agreement with those obtained from EPR. The irreversibility of the ZFC/FC curves observed at temperatures below the maximum of the ZFC curve for samples with $x \geqslant 0.87$ is a finger-print of spin-glass behaviour. The divergent tendency of the nonlinear susceptibility (χ_{nl}) when approaching T_m from above has been interpreted as evidence of a spin-glass phase transition. Static scaling analysis of χ_{nl} data has been carried out, yielding critical exponents comparable with those obtained for other spin glasses with short-range interactions where the random distribution of magnetic ions plays the main role.

Acknowledgments

The authors thank Dr G F Goya for helpful discussions. This work was supported in part by the Brazilian agencies CNPq and FAPESP. One of us (JAHC) thanks FINATEC for the financial support.

References

[1] Dietl T 1994 *Handbook on Semiconductors* vol 3b, ed T S Moss (Amsterdam: North-Holland) p 1251
[2] Furdyna J K 1986 *J. Vac. Sci. Technol.* A **4** 2002
[3] Nikiforov K G 1999 *Prog. Cryst. Growth Charact. Mater.* **39** 1
[4] Woolley J C, Bass S, Lamarcha A M, Lamarche G, Quintero M, Morocoima M and Bocaranda P 1995 *J. Magn. Magn. Mater.* **150** 553
[5] Morón M C and Hull S 2001 *Phys. Rev.* B **64** 220402
[6] Mydosh J A 1993 *Spin Glasses: an Experimental Introduction* (London: Taylor and Francis)
[7] Chowdhury D 1986 *Spin Glasses and Other Frustrated System* (Singapore: World Scientific)
[8] Canella V, Mydosh J A and Budnick J 1971 *J. Appl. Phys.* **42** 1689
[9] Tholence J L, Benoit A, Mauger A, Escorne M and Triboulet R 1984 *Solid State Commun.* **49** 417
[10] Kennett M P 2002 *Thesis Dr.* University of Boston USA
[11] Binder K and Schroder K 1976 *Phys. Rev.* B **14** 2141
Binder K and Young A P 1986 *Rev. Mod. Phys.* **58** 801
[12] Villain J 1979 *Z. Phys.* B **19** 1610
[13] Range K J, Klement U, Döll G, Bucher E and Baumann J R 1991 *Z. Naturf.* b **46** 1122
[14] Schäfer H 1964 *Chemical Transport Reactions* (New York: Academic)
[15] Döll G, Luxsteiner M C, Kloc C, Baumann J R and Bucher E 1990 *J. Cryst. Growth.* **104** 593
[16] Mantilla J 2004 *Thesis Dr.* University of São Paulo Brasil
Mantilla J, Brito G E S, ter Haar E, Sagredo V and Bindilatti V 2004 *J. Phys.: Condens. Matter* **16** 3555
[17] Mantilla J, Bindilatti V, Ter Haar E, Coaquira J A H, Brito G E S, Gratens X and Sagredo V 2004 *J. Magn. Magn. Mater.* **272–276** 1308
[18] Viticoli S 1986 *Prog. Cryst. Growth Chem.* **13** 105
[19] Spalek J, Lewicki A, Tarnawski Z, Furdyna J K, Galazka R R and Obuszko Z 1986 *Phys. Rev.* B **33** 3407
[20] Shapira Y, McNiff E J, Oliveira N F, Honig E D, Dwight K and Wold A 1988 *Phys. Rev.* B **37** 411
[21] Goya G and Sagredo V 2001 *Phys. Rev.* B **64** 235208
[22] Mantilla J, Pontuschka W M, Gamarra L, Salvador V L, Couto S G, Costa-Filho A J, Brito G E S, Sagredo V and Bindilatti V 2005 *J. Phys.: Condens. Matter* **17** 2755
[23] Sagredo V, ter Haar E and Attolini G 2002 *Physica* B **320** 407
[24] Pekarek T M, Watson E M, Garner J, Shand P M, Miotkowski I and Ramdas A K 2007 *J. Appl. Phys.* **101** 09D511
[25] Sagredo V, Morón M C, Betancourt L and Delgado G E 2007 *J. Magn. Magn. Mater.* **312** 294
[26] Mantilla J, ter Haar E, Coaquira J A H and Bindilatti V 2007 *J. Phys.: Condens. Matter* **19** 386225
[27] Ferre J, Rajchenbach J and Maletta H 1981 *J. Appl. Phys.* **52** 1829
[28] Campos J 1995 *Thesis Dr.* University of Zaragoza

[29] Börgermann F J, Maletta H and Zinn W 1986 *J. Magn. Magn. Mater.* **54–57** 71
[30] McAlister S P, Furdyna J K and Giriat W 1984 *Phys. Rev.* B **29** 1310
[31] Lähderanta E, Laiho R, Eftimova K and McGuire J J 2000 *Physica* B **284–288** 1343
[32] Labarta A, Batlle X, Martínez B and Obredors X 1992 *Phys. Rev.* B **46** 8994
[33] Eftimova K, Laiho R, Lähderanta E and Nordblad P 1997 *J. Magn. Magn. Mater.* **166** 179
[34] Suzuki M 1977 *Prog. Theor. Phys.* **58** 1151
[35] Chalupa J 1977 *Solid State Commun.* **22** 315
[36] Barbara B, Malozemoff A P and Imry Y 1981 *Phys. Rev. Lett.* **47** 1852
[37] Martínez B, Labarta A, Rodríguez-Solá R and Lobradors X 1994 *Phys. Rev.* B **50** 15779
[38] Eftimova K and McGuire J J 2000 *J. Phys.: Condens. Matter* **12** 1819
[39] Levi L P and Ogielski A T 1986 *Phys. Rev. Lett.* **57** 3288
Levi P M and Zhang Q 1986 *J. Magn. Magn. Mater.* **54–57** 133
[40] Ogielski A T and Morgenstern I 1985 *Phys. Rev. Lett.* **54** 928
[41] Haake F, Lewestein M and Wilkens M 1987 *Z. Phys.* B **66** 201